Check for updates

Original Research Article

Tanshinone Improves Endoplasmic Reticulum Stress Injury in Mice with Ischemic Cerebral Infarction by Regulating miR-29 and Inhibiting PI3K/Akt Signaling Pathway

Pharmacognosy Magazine
22(4) 1402–1412, 2026
© The Author(s) 2026
Article reuse guidelines:
in.sagepub.com/journals-permissions-india
DOI: 10.1177/09731296251404218
journals.sagepub.com/home/phm

Bo Xiong[1], Jianju Zhou[2], Hang Li[1] and Yuanchao Wen[1]

Abstract

Background: Tanshinone (TSL) is a good traditional Chinese medicine with a wide range of applications. Whether it plays a role in ischemic cerebral infarction is unclear.

Objectives: This study aims to explore the mechanism of tanshinone (TSL) to improve endoplasmic reticulum stress injury in mice with ischemic cerebral infarction by regulating miR-29 and inhibiting the phosphatidylinositol 3-kinase/protein kinase B (PI3K/Akt) signaling pathway.

Materials and Methods: Ischemic cerebral infarction mouse models were constructed and divided into the NC group, TSL group, TSL+miR-29mimic group, and TSL+miR-29inhibitor group. The expression of P-EIF-2α and P-PERK in the ischemic penumbra cortical area of cerebral infarction lesions was monitored, brain cell apoptosis was observed, and genes related to the miR-29 and PI3K/Akt pathways in the tissue were detected.

Results: A cerebral infarction model was successfully prepared. Compared with the sham operation group, the cerebral infarction site was severely ischemic and larger; TSL had an improved effect on ischemic cerebral infarction, and polydopamine-based nanoparticles (PDA NPs)-TSL had the best effect; TSL can reduce the expression of P-PERK in the cortical area and inhibit the expression of P-EIF-2α in the cortical area of the ischemic penumbra, and TSL has a more significant effect in this aspect. By using agonists and inhibitors of miR-29, TSL promotes the expression of miR-29 and improves endoplasmic reticulum stress injury in mice with ischemic cerebral infarction by inhibiting the PI3K/Akt signaling pathway.

Conclusion: TSL has a good anti-inflammatory effect, can reduce the expression of P-PERK in the cortical area, inhibit the expression of P-EIF-2α in the ischemic penumbra cortical area, and inhibit PI3K/Akt signaling by promoting miR-29 pathway to improve endoplasmic reticulum stress damage in mice with ischemic cerebral infarction.

Keywords

Polydopamine nanoparticles, tanshinone, miR-29, PI3K/Akt, ischemic cerebral infarction, endoplasmic reticulum stress, injury

Received 17 January 2025; **revised** 25 March 2025; **accepted** 17 September 2025

Introduction

Tanshinone (TSL) is a good traditional Chinese medicine with a wide range of applications. TSL can inhibit the excitotoxicity of glutamate and reduce neuronal death. In addition, TSL can regulate autophagy to a certain extent, promote the formation and degradation of autophagosomes, and protect neurons from damage by autophagy disorders (Li, Huang, et al., 2022). It inhibits the nuclear factor-κB (NF-κB) signaling pathway, thereby reducing damage to brain cells caused by inflammatory reactions; therefore, the good biological effects of TSL are the basis for its further in-depth research. Studies have found that Panax notoginseng total saponins can reduce endoplasmic reticulum stress damage caused by ischemic cerebral infarction, reduce the expression of endoplasmic reticulum stress-related proteins such as GRP78 and CHOP, and protect nerve cells from endoplasmic reticulum stress (Lou et al., 2020). Burdock may inhibit the activation of the PERK signaling pathway and block the activation of PERK, thereby reducing the expression of the transcription factor CHOP, thereby reducing cell damage caused by

Bo Xiong and Jianju Zhou contributed equally to this work.
[1]Department of Neurosurgical Center—Cerebrovascular Disease, Zunyi First People's Hospital, Zunyi, Guizhou, China
[2]Department of Neurological Rehabilitation, Zunyi First People's Hospital, Zunyi, Guizhou, China

Corresponding author:
Bo Xiong, Department of Neurosurgical Center—Cerebrovascular Disease, Zunyi First People's Hospital, Zunyi, Guizhou 563099, China.
E-mail: 13984514419@163.com

Creative Commons Non Commercial CC BY-NC: This article is distributed under the terms of the Creative Commons Attribution-NonCommercial 4.0 License (http://www.creativecommons.org/licenses/by-nc/4.0/) which permits non-Commercial use, reproduction and distribution of the work without further permission provided the original work is attributed as specified on the SAGE and Open Access pages (https://us.sagepub.com/en-us/nam/open-access-at-sage).

endoplasmic reticulum stress and improving the survival rate of nerve cells. In addition, matrine can reduce the level of reactive oxygen species (ROS) produced in cells by regulating the IRE1 signaling pathway, thereby alleviating endoplasmic reticulum stress damage in brain cells (Chen et al., 2016). These have laid a solid foundation for the important treatment of brain diseases. Although traditional Chinese medicine has a positive effect in treating endoplasmic reticulum stress injury in ischemic cerebral infarction, the role and mechanism of TSL in this aspect are not yet clear and remain to be studied.

In neurodevelopmental disorders, miR-29 is abnormally expressed (Hu et al., 2021), which can regulate the expression of synapse-related genes such as Atg5, Atg7, and Beclin-1, affecting the formation and function of synapses and regulating neuronal apoptosis and autophagy processes, thereby affecting the survival and development of neurons; it can also target genes such as ULK1 and ATG13 (Li, Deng, et al., 2022), thereby inhibiting the initiation process of autophagy to inhibit the occurrence and development of autophagy. Studies have pointed out (Li et al., 2017) that this gene can also target ULK1 and ATG13 to achieve autophagy inhibition. Studies have shown (Li et al., 2017) that miR-29 can not only target tumor necrosis factor-alpha (TNF-α) but also regulate TLR4 and MyD88 and has an inhibitory effect on the activation of microglia and inflammatory responses. In addition, miR-29 can directly target blood–brain barrier-related genes such as Claudin-5 and Occludin, inhibit their effect on increasing the permeability of the blood-brain barrier, and inhibit the occurrence and development of brain inflammation and edema (Liu et al., 2021). The above studies indicate that miR-29 plays an important role in improving endoplasmic reticulum stress in ischemic cerebral infarction. These studies show that miR-29 plays a crucial role in improving endoplasmic reticulum stress in ischemic cerebral infarction. In addition, studies believe (Tong et al., 2020) that inhibiting the PI3K/Akt signaling pathway can increase the activity of FOXO, promote the expression of mitochondrial antioxidant enzymes such as MnSOD and GPx, reduce the phosphorylation of Prx1, and enhance its reducing activity, thereby increasing the cell's response to ROS. The scavenging ability reduces ROS production. In addition, inhibiting the PI3K/Akt signaling pathway can regulate the expression and function of Calbindin-D28k to enhance the buffering capacity of Ca^{2+} in the cytoplasm, thereby reducing Ca^{2+} loss to a certain extent (Wang et al., 2019) and helping to maintain intracellular calcium homeostasis. This can protect the structure and function of the endoplasmic reticulum and reduce cell death caused by stress damage to the endoplasmic reticulum. Although the PI3K/Akt signaling pathway plays an important role in improving endoplasmic reticulum stress, it is unclear whether it is regulated by TSL and miR-29 to improve endoplasmic reticulum stress damage in mice with ischemic cerebral infarction, and needs further exploration. However, when decomposed and metabolized in the human body, some by-products and metabolites will be produced, which will bring adverse reactions and toxic side effects to the human body (Huang et al., 2020). Moreover, when the drug is taken orally, it will be metabolized by the human digestive system and liver, allowing the drug to achieve its goal. The number of organizations decreases (Wu et al., 2018).

Materials and Methods

Instruments, Reagents, and Animals

TSL (Shaanxi Haochen Biotechnology Ltd.); isoflurane (Wuhan Xinxinjiali Biotechnology Co., Ltd.); lidocaine (Jiangsu Ruidian Pharmaceutical Co., Ltd.); dopaquinoline monomer (Chengdu Bokochenxin Pharmaceutical Ltd.); PI3K antibody (Shanghai Yaji Biotechnology Co., Ltd.); AKT antibody (Wuhan Fenn Biotechnology Co., Ltd.); p-AKT antibody (Shanghai Yubo Biotechnology Co., Ltd.).

This study was approved by the ethics committee of the First Affiliated Hospital of Hebei North University.

Methods

Construction and Grouping of Ischemic Cerebral Infarction Mouse Models

Twenty-four rats, three of which were controls, were not subjected to any intervention. The remaining rats were anesthetized using 2.5% isoflurane and an oxygen flow of approximately 1.5 L/min. A scalpel was used to incise the head of the mouse. Shave the hair to one side of the midline of the head. Sterilize the skin and then make a skin incision of approximately 1 cm. Infiltrate the tissue around the incision with lidocaine local anesthetic and carefully expose the skull using a scalpel and forceps. Use a bone polisher to drill a hole slowly, about 1 mm in diameter, on the right side of the skull. Then, slowly pass a silicone thread through the perforation hole, extended to the blood supply area of the middle cerebral artery, and leave in place for 30 min. Slowly pull out the suture bolt, close the incision, clean the skin, and use temperature control equipment to maintain stable body temperature of the mouse. After 24 h, the mouse brain sections were stained with triphenyl tetrazolium chloride (TTC) dye to produce obvious cerebral infarction areas, which indicates that the required model has been successfully constructed. They were further divided into five groups, namely, NC group, TSL group, TSL+miR-29mimic group, and TSL+miR-29inhibitor group.

Determination of Brain Tissue Water Content

Anesthetize mice with 10% isoflurane, remove the diseased brain tissue, and quickly remove external blood and other tissues. Weigh the removed mouse brain tissue and record it as W1. Put the brain tissue into a drying oven preheated to

105°C to dry for 24 h. Maintain appropriate ventilation, and check and stir the sample regularly. Dry and cool. Weigh the dried sample and dish (W2). Moisture content (%) = [(W1 – W2)/W1] × 100.

Neurological Function Score (mNSS)

After 1 week of continuous administration, mNSS was used to score mice in seven groups. Scoring criteria: Neuropathological gait score (0–3 points): 0 points indicate normal gait, and 3 points indicate severely abnormal gait. Thousands of drop tests (0–3 points): 0 means normal walking and balance, 3 means unable to walk or loses balance. Stab test: 0 and 2 points correspond to normal reaction and no reaction. Edge hook test (0–3 points): 0 points means normal walking and grasping; 3 points means inability to walk or difficulty grasping. Add the four ratings above to get a total score (Ripa et al., 2017). The lowest score is 0 (no neurological deficit), and the highest score is 11 (most severe neurological deficit).

TTC Staining Method to Determine the Infarct Volume of Mouse Brain Tissue

Kill the mice and quickly remove the brains. After rapid freezing, remove the brain tissue slices and cut them into 2 mm brain slices with a clean blade. Add 2% TTC solution and a constant temperature of 37°C. Box, stain for 15–30 min, take out the stained brain slices, place them on a flat surface, take images of the brain slices, and use ImageJ to analyze the samples in each group and measure the infarct area.

qRT-PCR Detection

Total RNA was extracted using the TRIzol method and reverse transcribed into cDNA. The results of this method were verified using SYBR fluorescent PCR technology. Glyceraldehyde 3-phosphate dehydrogenase (GAPDH) is an intrinsic control between ROCK/MLCK and miRNA, and the qRT-PCR results were analyzed. Relative expression levels were estimated using the $2^{-\Delta\Delta Ct}$ method. Table 1 lists the primers and primer sequences.

Western Blot

Cells were extracted and digested in a lysis buffer, and their total protein content was measured. Separate by 10% sodium dodecyl sulfate-polyacrylamide gel electrophoresis (SDS-PAGE) and then incubated with primary antibody at 4°C overnight. Wash and incubate the membrane with horseradish peroxidase (HRP)-labeled secondary antibody for 1 h. Detection was enhanced by the internal reference GAPDH.

Enzyme-linked Immunosorbent Assay (ELISA) Method to Detect Inflammatory Factor Levels

The samples from each group were anesthetized, and the abdominal aorta blood was taken. The expression of interleukin-1β (IL-1β), tumor necrosis factor-alpha (TNF-α), interleukin-16 (IL-16), and other inflammatory factors in blood was detected according to the instructions of the kit.

TUNEL Detects Neuronal Cell Apoptosis

Six-well plate, trypsin digestion. After completion, transfer it to an EP tube, start centrifugation, wash thoroughly with phosphate-buffered saline (PBS) solution three times after centrifugation, and then fix it with an appropriate amount of 75% ethanol solution; leave it overnight, and add start incubating with an appropriate amount of RNase solution. After half an hour, add propidium iodide (PI) staining solution, incubate in a dark environment, and use the FACSCalibur flow cytometer for detection.

Statistical Methods

The data obtained in each of the above experiments were analyzed using SPSS 21.0 and GraphPad Prism software. If there are no special requirements, $p < .05$ is used as the test standard.

Table 1. Real-time PCR Primers and Primer Sequences.

	Primer	Sequences
miR-29	Forward primer	5′-TGTGAATCAGTGCAGGGTCC-3′
	Reverse primer	5′-CAGTGCAGGGTCCGAGGG-3′
PI3K	Forward primer	5′-GAAAAGGCCAGGTTGAACTG-3′
	Reverse primer	5′-ATGGTTGGCCTCGGGAATTT-3′
Akt	Forward primer	5′-ACCCAGCTACGACCAAAATG-3′
	Reverse primer	5′-TCCACAAGACCATTGGTTCA-3′
GAPDH	Forward primer	5′-TGTGTCCGTCGTGGATCTGA-3′
	Reverse primer	5′-CCTGCTTCACCACCTTCTTGAT-3′

Results

Successful Modeling of Ischemic Cerebral Infarction

The cerebral infarction model was successfully prepared. Compared with the sham operation group, the cerebral infarction site was severely ischemic and larger (Figure 1). The expression of P-PERK in the ischemic penumbra was further observed. Immunohistochemistry found that the number of positive cells in the model group increased abnormally in the hippocampal neuron cytoplasm and axon dendrites (Figure 2).

TSL Can Improve Ischemic Cerebral Infarction, and TSL Has the Best Effect

Observing the biological effects of TSL found that although TSL can reduce the volume of infarct lesions in ischemic cerebral infarction (Figure 3), observation of brain tissue cells found that TSL can effectively reduce ischemic cerebral infarction in mice. Cell apoptosis rate and TSL have a more significant effect in this aspect (Figure 4); TSL can reduce the expression of P-PERK in the cortical area (Figure 5), and inhibit P in the ischemic penumbra cortical area -EIF-2α expression (Figure 6), and the effect of TSL in this aspect is more significant.

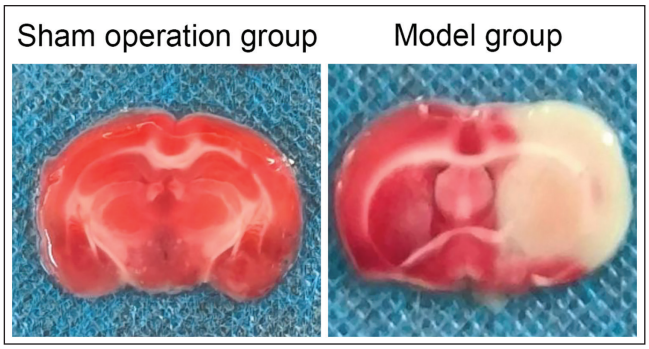


Figure 1. Cerebral Infarction Tissue Volume of Mice in the Modeling Group.

TSL Improves Endoplasmic Reticulum Stress Injury in Mice with Ischemic Cerebral Infarction by Promoting the Expression of miR-29, Which is Related to the Phosphorylation of the PI3K/Akt Signaling Pathway

Further observation of the levels of inflammatory factors in the brain tissue of mice found that the intervention of TSL reduced the levels of TNF-α and interleukin-6 (IL-6) in the brain tissue of mice to the greatest extent, and the TSL group showed a downward trend. More significantly (Figure 7A-7C), the NC group has the lowest expression level of miR-29, while under TSL and TSL intervention conditions, the expression level increases (Table 2), and the PI3K/Akt pathway genes also show the opposite. According to the trend, further comparison showed that TSL had the strongest intervention effect ($p < .05$). The expression of caspase-3 and Bcl-2 genes was reduced to a certain extent, while Bax showed a significantly increased trend (Table 3).

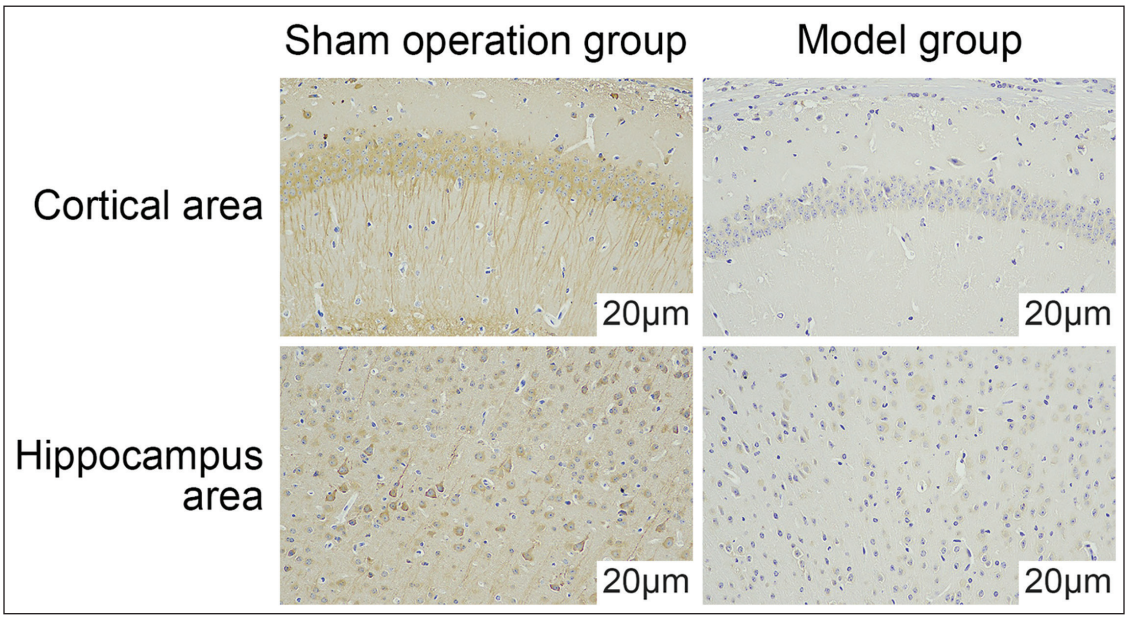


Figure 2. P-PERK Expression in Ischemic Penumbra. Arrows Show the Ischemic Area.

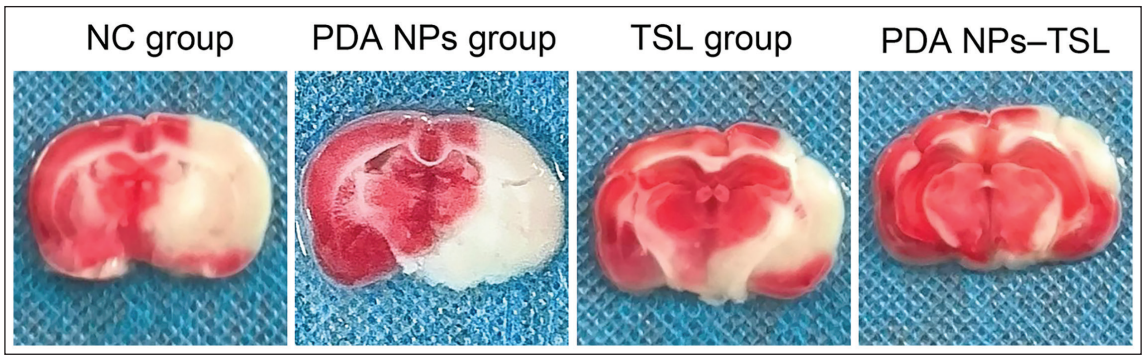


Figure 3. Volume of Cerebral Infarction Tissue in Mice.

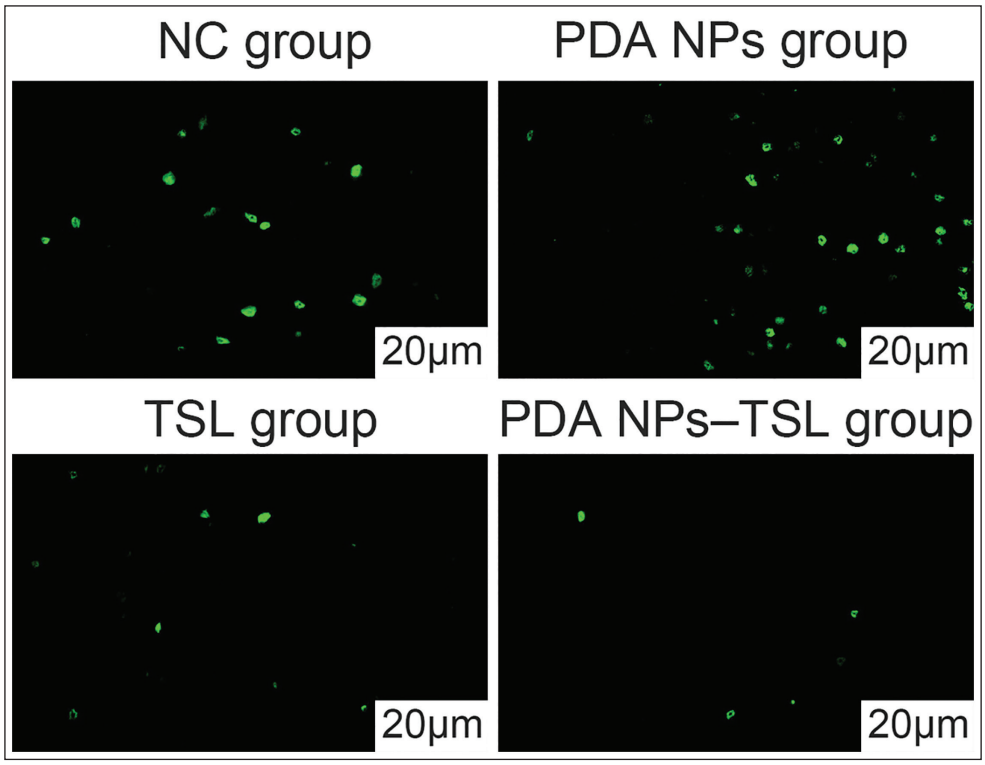


Figure 4. TUNEL Detects Apoptosis in Brain Tissue.

TSL Improves Endoplasmic Reticulum Stress Injury in Mice with Ischemic Cerebral Infarction by Inhibiting the PI3K/Akt Signaling Pathway

We performed different interventions on the basis of the NC group. By using agonists and inhibitors of miR-29, we found that under the intervention of miR-29mimic, the levels of inflammatory factors in the brain tissue of mice were significantly reduced compared with the NC group (Table 4). In contrast, the miR-29inhibitor group showed opposite results. At the same time, under the combined intervention of TSL and miR-29mimic, the levels of related inflammatory factors were lower than those using miR-29mimic alone (Figure 8A–8C). Through the observation of the relative gene expression levels of miR-29, it was found that TSL can promote the expression of miR-29mimic. It shows that TSL can improve endoplasmic reticulum stress damage in mice with ischemic cerebral infarction by promoting the expression of miR-29. In addition, during this experiment, we found that TSL inhibited the expression of PI3K and Akt, and the inhibitory effect was the most obvious in the TSL+miR-29mimic group. This suggests that the effect of TSL on promoting the expression of miR-29 and improving endoplasmic reticulum stress injury in mice with ischemic cerebral infarction is achieved by inhibiting the PI3K/Akt signaling pathway.

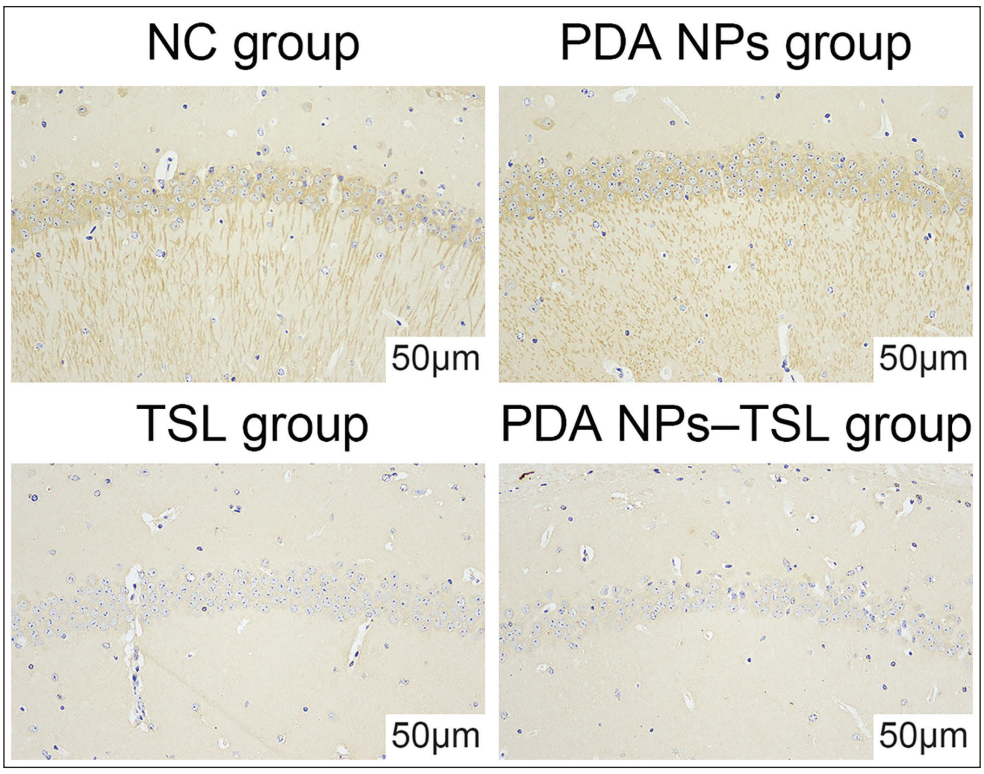


Figure 5. P-PERK Expression in the Ischemic Penumbra Cortical Area. Arrows Show the Ischemic Area.

Discussion

TSL is an active ingredient widely used in Chinese herbal medicine. It has various pharmacological effects, such as anti-platelet aggregation, anti-coagulation, and improvement of microcirculation. Research has shown (Vera et al., 2021) that TSL can inhibit the activation of IKK, thereby blocking the NF-κB signaling pathway to the greatest extent, hindering the degradation of IκB protein, and thereby maintaining its interaction with NF-κB. The purpose of binding is to inhibit the transcriptional activity and nuclear translocation of NF-κB and, at the same time, increase the nuclear translocation of Nrf2 and enhance its activity, thereby inhibiting macrophages from producing TNF-α, IL-1β, IL-6, and other (Vera et al., 2021) inflammatory factors, reducing oxidants such as ROS and nitric oxide (NO), thereby alleviating oxidative stress. However, according to practical applications, the poor water solubility of TSL leads to the instability of its efficacy, which in turn limits its clinical application (Sassi et al., 2017). Therefore, using polydopamine nanoparticles as carriers and encapsulating TSL can improve its solubility and stability, making it easier to deliver and absorb in the body, thereby improving its efficacy and reducing toxic side effects. In addition, polydopamine nanoparticles can increase drug loading and coating efficiency, thereby improving the bioavailability and therapeutic effect of TSL (Huang et al., 2022; Ru et al., 2016). In this study, we successfully prepared TSL composites and used for further animal experiments. In order to explore the effect of TSL on ischemic cerebral infarction, through observation of pathological brain tissue sections, it was found that TSL can effectively reduce the cell apoptosis rate in mice with ischemic cerebral infarction, and TSL has a more effective effect in this regard. Significantly, further observation of the levels of inflammatory factors in the mouse brain tissue found that the intervention of TSL significantly reduced the levels of TNF-α and IL-6 in the mouse brain tissue, and the TSL group showed a downward trend. More significantly, it shows that TSL has good anti-inflammatory and inhibitory brain cell apoptosis value, can enhance the stability and targeting of TSL, and improve its concentration and action time at the site of ischemic cerebral infarction, thereby enhancing neuroprotection.

P-PERK and P-EIF-2α are key molecules in the endoplasmic reticulum stress response (Chandiran et al., 2018) and are involved in regulating processes such as protein synthesis and apoptosis. Activated P-PERK inhibits protein synthesis by phosphorylating EIF-2α (Wang et al., 2022) thereby reducing endoplasmic reticulum load; phosphorylation of P-EIF-2α reduces its binding ability to GTP, making it difficult for the translation initiation complex to form, thereby inhibiting protein synthesis, which is a cell self-protection mechanism (Yang et al., 2018), which can reduce the load of the endoplasmic reticulum by reducing protein synthesis. Under endoplasmic reticulum stress, P-PERK can also upregulate the

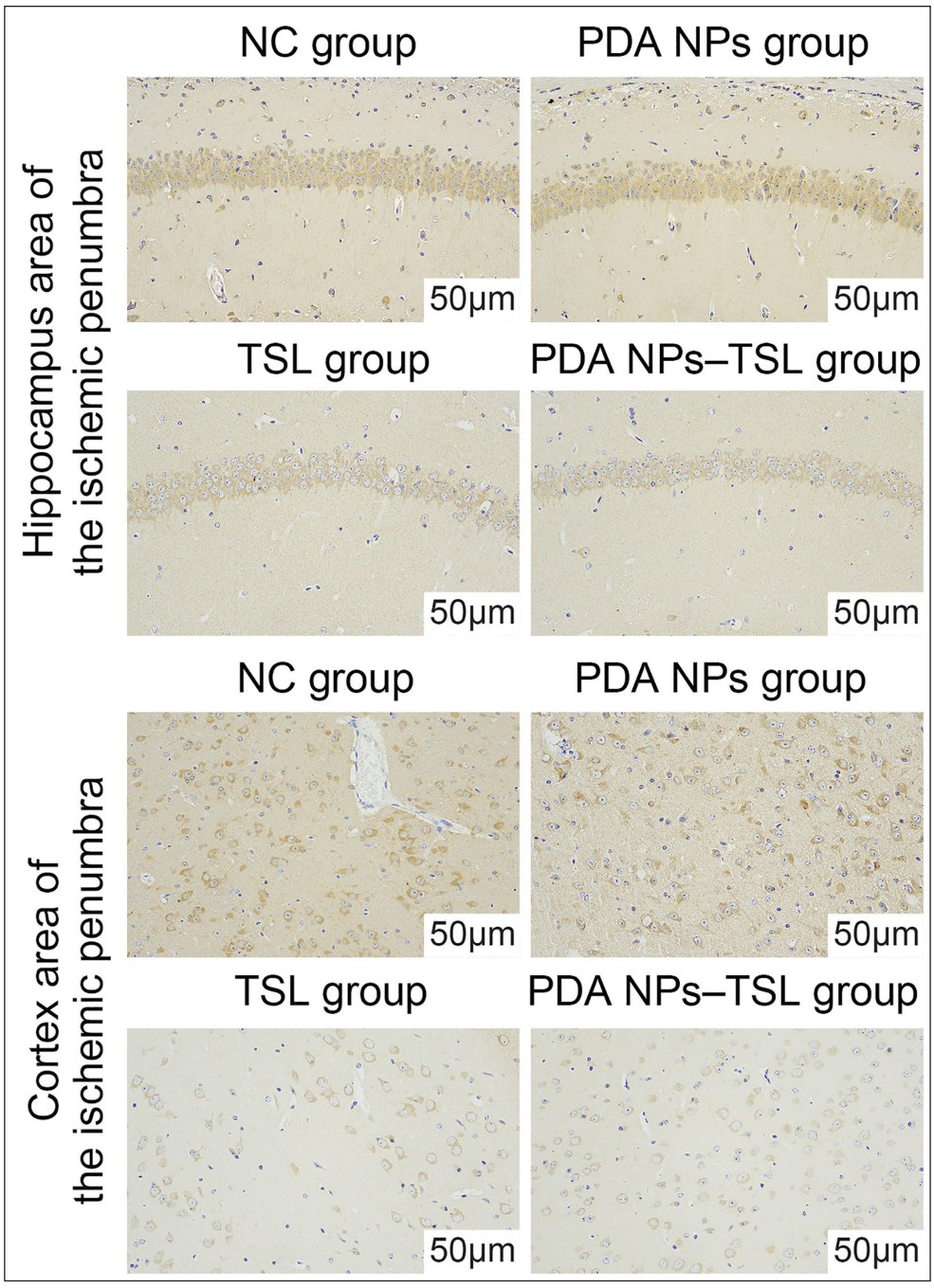


Figure 6. P-EIF-2α Expression in the Cortex Area and Hippocampus Area of the Ischemic Penumbra.

expression of a series of stress response genes, including molecular chaperones, antioxidant enzymes, and proteasomes, by activating ATF4 to help cells cope with endoplasmic reticulum stress. Further research results show that TSL and TSL can reduce the expression of P-PERK in the cortical area and inhibit the cell damage and apoptosis caused by P-EIF-2α in the endoplasmic reticulum stress response in the cortical area of the ischemic penumbra. It has an inhibitory effect on various aspects, and at the same time, its antioxidant and regulating effects on endoplasmic reticulum stress response are greatly improved.

In further experiments, TSL activated the I3K/Akt pathway, which improved the levels of inflammatory factors such as TNF-α and IL-6 to a certain extent, thus promoting the survival and differentiation of neurons and exerting its neuroprotective effect. During this process, miR-29 is significantly promoted. Analysis suggests that miR-29 can inhibit the expression of the SOD2 gene (Lyu et al., 2018), thereby

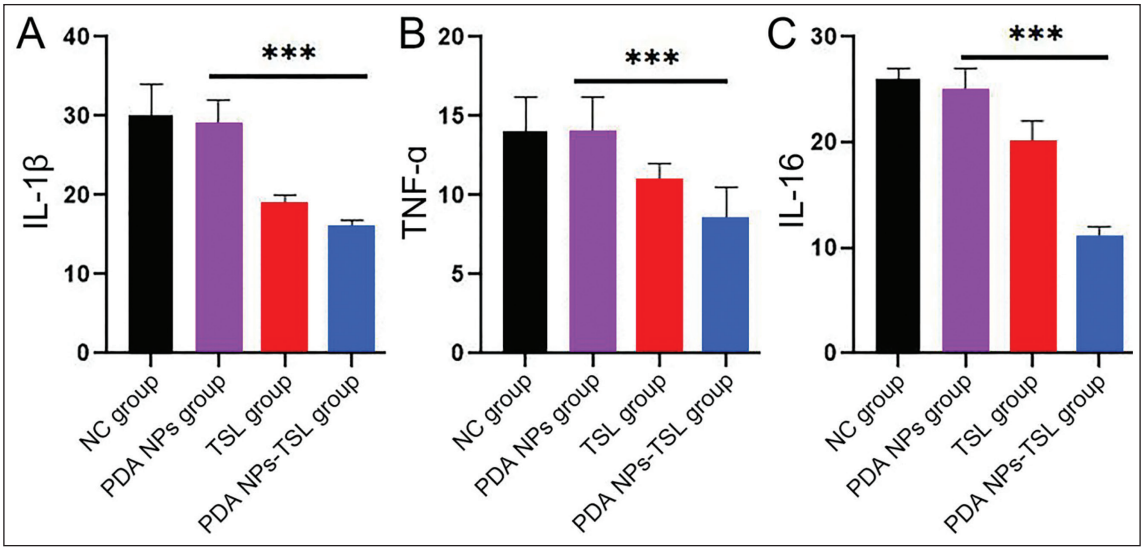


Figure 7. Levels of Inflammatory Factors in Brain Tissue in Each Group. (A) Interleukin-1β (IL-1β); (B) Tumor Necrosis Factor-alpha (TNF-α); (C) Interleukin-6 (IL-6).

Note: *P <0.001.

Table 2. Changes in miR-29 and PI3K/Akt Signaling Pathways.

Group	miR-29	PI3K	AKT	p-AKT
Normal group	0.99 ± 0.07	0.94 ± 0.16	0.90 ± 0.05	1.31 ± 0.15
Sham operation group	0.95 ± 0.05	0.91 ± 0.12	0.88 ± 0.06	1.24 ± 0.04
NC group	0.55 ± 0.04*	1.04 ± 0.11*	0.94 ± 0.06*	1.43 ± 0.07*
PDA NPs group	0.54 ± 0.12*	1.03 ± 0.12*	1.02 ± 0.06*	1.38 ± 0.04*
TSL group	0.94 ± 0.07*#	0.85 ± 0.08*	0.72 ± 0.09*	0.72 ± 0.09*
PDA NPs-TSL group	1.23 ± 0.05*#	0.77 ± 0.07*#	0.68 ± 0.04*#	0.40 ± 0.08*#
F value	5.863	11.942	9.427	8.391
p value	<.001	<.001	<.001	<.001

Note: Compared with sham operation group, *p <0.05; compared with PDA NPs group, #p <0.05.

Table 3. Expression Levels of Apoptosis-related Genes.

Group	Caspase-3	Bcl-2	Bax
Normal group	0.98 ± 0.10	0.87 ± 0.13	0.97 ± 0.03
Sham operation group	0.91 ± 0.06	0.83 ± 0.02	1.00 ± 0.04
NC group	1.30 ± 0.09*	0.56 ± 0.09*	1.40 ± 0.06*
PDA NPs group	1.26 ± 0.14*	0.61 ± 0.07*	1.31 ± 0.07*
TSL group	1.13 ± 0.12*#	0.74 ± 0.05*#	1.02 ± 0.16*#
PDA NPs-TSL group	1.08 ± 0.04*#	0.79 ± 0.03*#	1.11 ± 0.12*#
F value	6.321	4.783	7.042
p value	<.001	.002	<.001

Note: Compared with sham operation group, *p <0.05; compared with PDA NPs group, #p <0.05.

Table 4. Changes in miR-29 and PI3K/Akt Signaling Pathways.

Group	miR-29	PI3K	AKT	p-AKT
NC group	0.55 ± 0.04*	1.04 ± 0.11*	0.94 ± 0.06	1.43 ± 0.07
TSL group	1.23 ± 0.05*#	0.77 ± 0.07*#	0.68 ± 0.04*#	0.40 ± 0.08*#
miR-29mimic group	1.89 ± 0.12*#	0.99 ± 0.13*#	1.04 ± 0.16*#	1.06 ± 0.16*#
miR-29inhibitor group	0.75 ± 0.03*	0.81 ± 0.05*	0.68 ± 0.14*	0.68 ± 0.12*
TSL+miR-29mimic group	2.04 ± 0.08*#	0.55 ± 0.07*#	0.47 ± 0.03*#	0.33 ± 0.05*#
TSL+miR-29inhibitor group	0.83 ± 0.14*	0.71 ± 0.02*#	0.73 ± 0.11*#	0.74 ± 0.03*#

Note: Compared with NC group, *p <0.05; compared with miR-29 inhibitor group or TSL+miR-29 inhibitor group, #p <0.05.

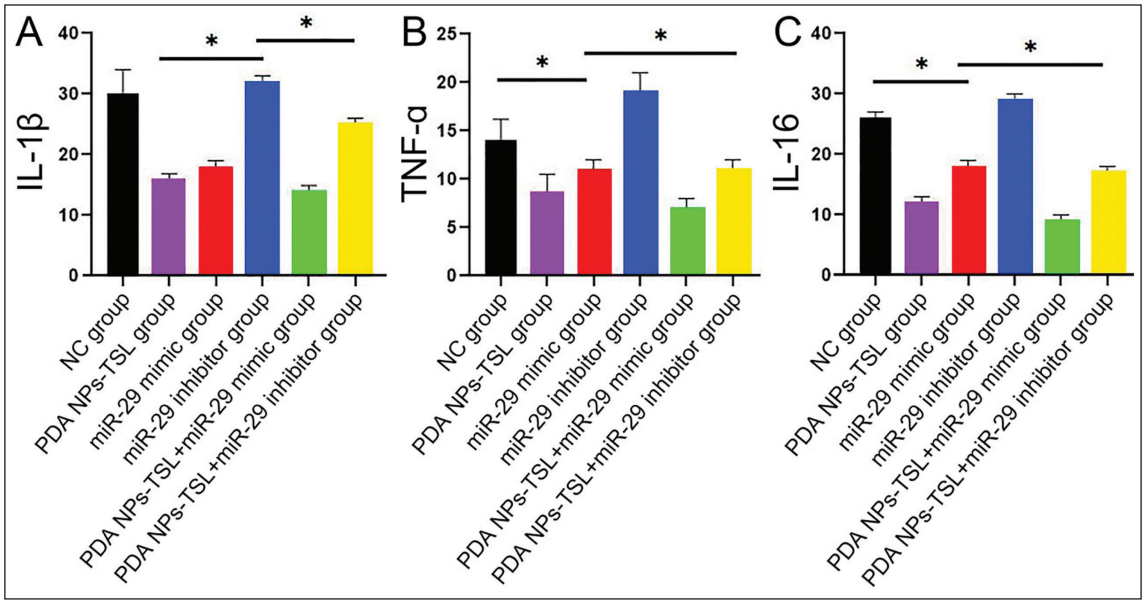


Figure 8. Inflammatory Factor Levels. *p < .05; ***p < .001. (A) Interleukin-1β (IL-1β); (B) Tumor Necrosis Factor-alpha (TNF-α); (C) Interleukin-6 (IL-6).

Note: *P <0.05.

reducing the scavenging capacity of intracellular superoxide anions and, at the same time, regulating the expression of antioxidant enzymes such as CAT and GPx, which further enhance the antioxidant capacity of cells. In addition, miR-29 can inhibit the expression of the Keap1 gene, thereby increasing the stability of Nrf2 in cells, initiating a series of transcription reactions, and increasing the transcription and expression of antioxidant genes such as HO-1, NQO1, and GCLC, thereby reducing oxidative damage (Lyu et al., 2018). TSL activates the expression of miR-29 and achieves the inhibitory effect on endoplasmic reticulum stress in brain cells in infarct lesions. In ischemic cerebral infarction, miR-29 reduces inflammation by inhibiting the expression of JAK and targeting STAT (Liu et al., 2022), thereby inhibiting the release of inflammatory factors such as IL-6 and TNF-α. The upregulation of miR-29 can inhibit the production and activation of NF-κB by binding to the mRNA of NF-κB and degrading its expression, thereby reducing the inflammatory response and related inflammatory damage. Research shows that miR-29 can promote p38 and JNK in the MAPK pathway at a certain level, inhibit PERK, and reduce the phosphorylation level of eIF2α to a certain extent, thereby reducing the production of XBP1s thereby blocking the endoplasmic reticulum response. The conduction of stimulating signals reduces cell damage (Dini et al., 2021). miR-29 can directly target the mRNA of PERK to inhibit its expression, thereby inhibiting the expression of PERK and endoplasmic reticulum stress. By using miR-29mimic, we found that it can significantly enhance the ameliorative effect of TSL on endoplasmic reticulum stress in ischemic cerebral infarction in mice. The miR-29inhibitor will reverse this effect. In addition, during the experiment, the expression of PI3K and Akt was significantly reduced due to the participation of miR-29mimic and TSL, and the result of co-intervention of miR-29mimic and TSL was the lowest level. It shows that the PI3K/Akt pathway is regulated during TSL treatment. This is because the PI3K/Akt

signaling pathway can promote nuclear translocation and increase the activity of the transcription factor Nrf2 through the activation of Akt (Hung et al., 2019), allowing it to bind to the ARE. On the other hand, it promotes the transcription and expression of SOD and GST (Gusti et al., 2021; Qi et al., 2017), thereby protecting cells from oxidative damage. This verified the mechanism of TSL improving endoplasmic reticulum stress damage in mice with ischemic cerebral infarction by promoting miR-29 and inhibiting the PI3K/Akt signaling pathway. The safe dosage and potency of polydopamine-based nanoparticles (PDA NPs)-TS need to be further explored in the future.

Conclusion

In summary, TSL can reduce the expression of P-PERK in the cortical area and inhibit the expression of P-EIF-2α in the cortical area of the ischemic penumbra. It can promote miR-29 to further effectively inhibit the PI3K/Akt pathway to achieve good results. It improves the effect of ischemic cerebral infarction in mice and regulates endoplasmic reticulum stress damage, which provides a foundation for the development of new drugs for ischemic cerebral infarction.

Abbreviations

EIF: Eukaryotic translation initiation factor; PDA NPs: Polydopamine-based nanoparticles; PI3K/Akt: Phosphatidylinositol 3-kinase/protein kinase B; TSL: Tanshinone.

Acknowledgments

This work was supported by the Zunshi Kehe HZ Zi (2024) No. 44-The study on the correlation between the construction and effectiveness of pre-hospital treatment systems for stroke patients.

Declaration of Conflicting Interests

The authors declared no potential conflicts of interest with respect to the research, authorship, and/or publication of this article.

Ethical Approval

This study was approved by the ethnic committee of Zunyi First People's Hospital.

Funding

The author(s) disclosed receipt of the following financial support for the research, authorship, and/or publication of this article: The authors received the Zunshi Kehe HZ Zi (2024) No. 44 financial support for the research.

Informed Consent

Not applicable.

ORCID iD

Bo Xiong https://orcid.org/0009-0004-5375-273X

References

Chandiran, K., Lawlor, R., Pannuti, A., Perez, G. G., Srinivasan, J., Golde, T. E., Miele, L., Osborne, B. A., & Minter, L. M. (2018). Notch1 primes CD4 T cells for T helper type I differentiation through its early effects on miR-29. *Molecular Immunology*, *99*, 191–198. https://doi.org/10.1016/j.molimm.2018.05.002

Chen, H. C., Chen, P. Y., Wu, M. J., Tai, M. H., & Yen, J. H. (2016). Tanshinone IIA modulates low density lipoprotein uptake via down-regulation of PCSK9 gene expression in HepG2 cells. *PLoS One*, *11*(9), e0162414. https://doi.org/10.1371/journal.pone.0162414

Dini, S., Zakeri, M., Ebrahimpour, S., Dehghanian, F., & Esmaeili, A. (2021). Quercetin-conjugated superparamagnetic iron oxide nanoparticles modulate glucose metabolism-related genes and miR-29 family in the hippocampus of diabetic rats. *Scientific Reports*, *11*(1), 8618. https://doi.org/10.1038/s41598-021-87687-w

Gusti, A. M. T., Qusti, S. Y., Alshammari, E. M., Toraih, E. A., & Fawzy, M. S. (2021). Antioxidants-related superoxide dismutase, catalase, glutathione peroxidase, glutathione-*S*-transferase, and nitric oxide synthase gene variants analysis in an obese population: A preliminary case-control study. *Antioxidants*, *10*(4), 595. https://doi.org/10.3390/antiox10040595

Hu, X. X., Zhang, J., Deng, L. L., Hu, H., Hu, J. J., & Zheng, G. H. (2021). Galactose-modified PH-sensitive niosomes for controlled release and hepatocellular carcinoma target delivery of tanshinone IIA. *AAPS PharmSciTech*, *22*(3), 96. https://doi.org/10.1208/s12249-021-01973-4

Huang, Y. P., Long, X., Tang, J. Y., Li, X. L., Zhang, X., Luo, C. Y., Zhou, Y., & Zhang, P. (2020). The attenuation of traumatic brain injury via inhibition of oxidative stress and apoptosis by tanshinone IIA. *Oxidative Medicine and Cellular Longevity*, *2020*, 4170156. https://doi.org/10.1155/2020/4170156

Huang, D., Xue, H. Y., Shao, W. H., Wang, X. X., Liao, H. J., & Ye, Y. Q. (2022). Inhibiting effect of miR-29 on proliferation and migration of uterine leiomyoma via the STAT3 signaling pathway. *Aging-Us*, *14*(3), 1307–1320.

Hung, Y. H., Kanke, M., Kurtz, C. L., Cubitt, R., Bunaciu, R. P., Miao, J., Zhou, L. Y., Graham, J. L., Hussain, M. M., Havel, P., Biddinger, S., White, P. J., & Sethupathy, P. (2019). Acute suppression of insulin resistance-associated hepatic miR-29 *in vivo* improves glycemic control in adult mice. *Physiological Genomics*, *51*(8), 379–389. https://doi.org/10.1152/physiolgenomics.00037.2019

Li, H. F., Han, W. J., Wang, H. Y., Ding, F., Xiao, L. Y., Shi, R. N., Ai, L. P., & Huang, Z. B. (2017). Tanshinone IIA inhibits glutamate-induced oxidative toxicity through prevention of mitochondrial dysfunction and suppression of MAPK activation in SH-SY5Y human neuroblastoma cells. *Oxidative Medicine and Cellular Longevity*, *2017*, 4517486. https://doi.org/10.1155/2017/4517486

Li, Y., Deng, X., Zhuang, W. L., Li, Y., Xue, H., Lv, X., & Zhu, S. Q. (2022). Tanshinone IIA down-regulates-transforming growth factor beta 1 to relieve renal tubular epithelial cell inflammation and pyroptosis caused by high glucose. *Bioengineered*, *13*(5), 12224–12236. https://doi.org/10.1080/21655979.2022.2074619

Li, W., Huang, T., Xu, S., Che, B., Yu, Y., Zhang, W., & Tang, K. (2022). Molecular mechanism of tanshinone against prostate

cancer. *Molecules*, *27*(17), 5594. https://doi.org/10.3390/molecules27175594

Liu, L. J., Gao, H. J., Wen, T., Gu, T., Zhang, S., & Yuan, Z. Y. (2021). Tanshinone IIA attenuates AOM/DSS-induced colorectal tumorigenesis in mice via inhibition of intestinal inflammation. *Pharmaceutical Biology*, *59*(1), 89–96. https://doi.org/10.1080/13880209.2020.1865412

Liu, C. C., Liu, L. A., Bo, J. L., Lu, X., Qu, D. H., Liu, G. H., Jiang, Z. Y., & Cai, L. (2022). Hypoxia-induced downregulation of miR-29 in renal tumor cells affects collagen IV subunit expression through multiple sites. *Biomedicines*, *10*(12), 3286. https://doi.org/10.3390/biomedicines10123286

Lou, G. H., Hu, W. M., Wu, Z. Q., Xu, H., Yao, H., Wang, Y., Huang, Q. W., Wang, B. J., Wen, L., Gong, D. Y., Chen, X. B., Shi, Y. P., Yang, L., Xu, Y. M., & Wang, Y. (2020). Tanshinone II A attenuates vascular remodeling through klf4 mediated smooth muscle cell phenotypic switching. *Scientific Reports*, *10*(1), 13858. https://doi.org/10.1038/s41598-020-70887-1

Lyu, G. L., Guan, Y. T., Zhang, C., Zong, L., Sun, L., Huang, X. K., Huang, L., Zhang, L. J., Tian, X. L., Zhou, Z. J., & Tao, W. (2018). TGF-β signaling alters H4K20me3 status via miR-29 and contributes to cellular senescence and cardiac aging. *Nature Communications*, *9*(1), 2560. https://doi.org/10.1038/s41467-018-04994-z

Qi, H. P., Liu, Y., Li, S. Z., Chen, Y. P., Li, L., Cao, Y. G., Mingyao, E., Shi, P. L., Song, C., Li, B. Y., & Sun, H. L. (2017). Activation of AMPK attenuated cardiac fibrosis by inhibiting CDK2 via p21/p27 and miR-29 family pathways in rats. *Molecular Therapy-Nucleic Acids*, *8*, 277–290. https://doi.org/10.1016/j.omtn.2017.07.004

Ripa, R., Dolfi, L., Terrigno, M., Pandolfini, L., Savino, A., Arcucci, V., Groth, M., Tozzini, E. T., Baumgart, M., & Cellerino, A. (2017). MicroRNA miR-29 controls a compensatory response to limit neuronal iron accumulation during adult life and aging. *BMC Biology*, *15*(1), 9. https://doi.org/10.1186/s12915-017-0354-x

Ru, P., Hu, P., Geng, F., Mo, X. K., Cheng, C. M., Yoo, J. Y., Cheng, X., Wu, X. N., Guo, J. Y., Nakano, I., Lefai, E., Kaur, B., Chakravarti, A., & Guo, D. L. (2016). Feedback loop regulation of SCAP/SREBP-1 by miR-29 modulates EGFR signaling-driven glioblastoma growth. *Cell Reports*, *16*(6), 1527–1535. https://doi.org/10.1016/j.celrep.2016.07.017

Sassi, Y., Avramopoulos, P., Ramanujam, D., Grüter, L., Werfel, S., Giosele, S., Brunner, A. D., Esfandyari, D., Papadopoulou, A. S., De Strooper, B., Hübner, N., Kumarswamy, R., Thum, T., Yin, X. K., Mayr, M., Laggerbauer, B., & Engelhardt, S. (2017). Cardiac myocyte miR-29 promotes pathological remodeling of the heart by activating Wnt signaling. *Nature Communications*, *8*(1), 1614. https://doi.org/10.1038/s41467-017-01737-4

Tong, W. J., Guo, J. H., & Yang, C. F. (2020). Tanshinone II A enhances pyroptosis and represses cell proliferation of HeLa cells by regulating miR-145/GSDMD signaling pathway. *Bioscience Reports*, *40*, Bsr20200259. https://doi.org/10.1042/Bsr20200259

Vera, O., Bok, I., Jasani, N., Nakamura, K., Xu, X. N., Mecozzi, N., Angarita, A., Wang, K. Z., Tsai, K. N. Y., & Karreth, F. A. (2021). A MAPK/miR-29 axis suppresses melanoma by targeting MAFG and MYBL2. *Cancers*, *13*(6), 1408. https://doi.org/10.3390/cancers13061408

Wang, X. P., Fan, J. B., Ding, X. M., Sun, Y. Y., Cui, Z. M., & Liu, W. (2019). Tanshinone I inhibits IL-1β-induced apoptosis, inflammation and extracellular matrix degradation in chondrocytes CHON-001 cells and attenuates murine osteoarthritis. *Drug Design Development and Therapy*, *13*, 3559–3568. https://doi.org/10.2147/Dddt.S216596

Wang, X. X., Liu, Y. N., Hou, H. Q., Shao, W. H., Huang, D., Hao, Z. H., Xue, H. Y., & Ye, Y. Q. (2022). miRNA-29 of aggravates myocardial infarction via inhibiting the PI3K/mTOR/HIF1α/VEGF pathway. *Aging-Us*, *14*(7), 3129–3142.

Wu, D. M., Wang, Y. J., Han, X. R., Wen, X., Li, L., Xu, L., Lu, J., & Zheng, Y. L. (2018). Tanshinone IIA prevents left ventricular remodelling via the TLR4/MyD88/NF-κB signalling pathway in rats with myocardial infarction (Retracted article. See vol. 25, pg. 1326, 2021). *Journal of Cellular and Molecular Medicine*, *22*(6), 3058–3072. https://doi.org/10.1111/jcmm.13557

Yang, J. Y., Gong, X. J., Yang, J., Ouyang, L. H., Xiao, R., You, X., & Ouyang, Y. L. (2018). Suppressive role of microRNA-29 in hepatocellular carcinoma via targeting IGF2BP1. *International Journal of Clinical and Experimental Pathology*, *11*(3), 1175–1185.